

See discussions, stats, and author profiles for this publication at: <https://www.researchgate.net/publication/231639457>

A General Law for Predictive Use of Thermoporosimetry as a Tool for the Determination of Textural Properties of Divided Media

ARTICLE *in* THE JOURNAL OF PHYSICAL CHEMISTRY B · JULY 2004

Impact Factor: 3.3 · DOI: 10.1021/jp048189e

CITATIONS

25

READS

18

4 AUTHORS, INCLUDING:



Manuel Grivet

University of Franche-Comté

36 PUBLICATIONS 203 CITATIONS

SEE PROFILE



Jean-Marie Nedelec

Ecole Nationale Supérieure de Chimie de Cle...

156 PUBLICATIONS 1,797 CITATIONS

SEE PROFILE

A General Law for Predictive Use of Thermoporosimetry as a Tool for the Determination of Textural Properties of Divided Media

Nicolas Billamboz,[†] Mohamed Baba,[‡] Manuel Grivet,[†] and Jean-Marie Nedelec^{*,§}

Laboratoire de Microanalyses Nucléaires Alain Chambaudet, UMR CEA, Université de Franche-Comté, 16 route de Gray, 25030 Besançon Cedex France, Laboratoire de Photochimie Moléculaire et Macromoléculaire, UMR CNRS 6505, Ecole Nationale Supérieure de Chimie de Clermont Ferrand et Université Blaise Pascal, 24 Avenue des Landais 63174 Aubière Cedex France, and Laboratoire des Matériaux Inorganiques, UMR CNRS 6002, Ecole Nationale Supérieure de Chimie de Clermont Ferrand et Université Blaise Pascal, 24 Avenue des Landais 63174 Aubière Cedex France

Received: April 26, 2004; In Final Form: June 7, 2004

Nanoporous silica gels with well-defined textural properties have been used to calibrate the thermoporosimetry technique with various aromatic solvents including *o*-, *m*-, and *p*-xylene, *p*-dichlorobenzene, 1,2,4-trichlorobenzene, and naphthalene. The calibration has been validated on a test alumina sample, and the results are in good agreement with the one derived from gas sorption. The data obtained for the three xylene isomers indicate a linear variation of T_p , the temperature of crystallization of the solvent inside the pore of size R_p , with T_0 , the normal crystallization temperature ($T_p = aT_0 + b$). A linear fit of these curves gives a constant value for the slope ($a \approx 1$), but the value of the intercept b depends strongly on the size of the pore. These fitting curves describe perfectly the behavior of the other solvents showing that extrapolation within a structure-related family of solvents is possible. The expression $b = -196.41/R_p$ is derived from the data collected for the xylene isomers, and the final expression $T_p = 1.02T_0 - 196.41/R_p$ can be used directly to predict the crystallization temperature of any solvent in a pore of size R_p . This general law is derived for benzene-substituted solvents. Nevertheless, this work provides the first evidence of a possible predictive use of thermoporosimetry without fastidious preliminary calibration. The solvents studied in this paper are particularly valuable for swelling of polyolefins.

1. Introduction

It has been known for a long time¹ that a solvent confined in the pores of a material experiences an important shift of its liquid to a solid transition temperature. It has also been observed that this shift, ΔT , is related to the size of the pore, R_p , in which the solvent is trapped.^{2–4} The knowledge of the $R_p(\Delta T)$ function allows then the determination of the size of the pore of a material by simply measuring ΔT for a given solvent.^{5–7} Theoretically, this method, called thermoporosimetry, is very attractive for the determination of pore size in materials. Actually, application of this technique is very simple, fast, inexpensive, and nondestructive. Soaking the porous material in the solvent and measuring the crystallization temperature by differential scanning calorimetry (DSC) is indeed enough to derive R_p .

Several examples in the literature illustrate the use of thermoporosimetry as a tool for pore size determination.^{8–13} These studies mainly focus on the use of water as solvent.

The main drawback of thermoporosimetry lies in the fact that, to be applied, it requires precise knowledge of the $R_p(\Delta T)$ and $W_a(\Delta T)$ functions, where W_a is the apparent enthalpy of

crystallization. Because of these important limitations, thermoporosimetry has not been applied so often yet.

In previous work, it has been shown that sol–gel-derived nanoporous silica gels can be used as standard materials for calibration of thermoporosimetry.^{14,15}

Our main interest in using thermoporosimetry comes from the discovery that polymers swollen with a solvent behave in a very similar way to rigid porous materials. In particular, the solvent trapped inside the polymeric network shows a shift of its crystallization temperature.¹⁶ Analogy between organic polymeric networks and rigid porous materials has then been proposed,¹⁷ demonstrating that thermoporosimetry is a very useful tool to study cross-linking in polymers. In effect, the size of the mesh of the polymeric network, which controls the value of ΔT , is directly related to the cross-linking level of the polymer itself.

Thermoporosimetry consequently becomes a unique tool for the study of cross-linking in polymeric networks. It then became necessary to develop calibration procedures and materials for solvents of interest to polymer chemistry.

In a previous paper,¹⁷ it has also been demonstrated that thermoporosimetry also allows the determination of the porous volume of solids and the swelling ratio of polymers.

The aim of the present work is to reach a further step in the use of thermoporosimetry and to demonstrate that the calibration step could be avoided in certain conditions.

The idea is to explore several solvents with similar chemical formulation and to derive a general law that could be used to predict the behavior regarding thermoporosimetry of unknown

* To whom correspondence may be addressed. E-mail: j-marie.nedelec@univ-bpclermont.fr. Phone: 00 33 (0)473407105. Fax: 00 33 (0)473407108.

[†] Université de Franche-Comté.

[‡] Laboratoire de Photochimie Moléculaire et Macromoléculaire, Ecole Nationale Supérieure de Chimie de Clermont Ferrand et Université Blaise Pascal.

[§] Laboratoire des Matériaux Inorganiques, Ecole Nationale Supérieure de Chimie de Clermont Ferrand et Université Blaise Pascal.

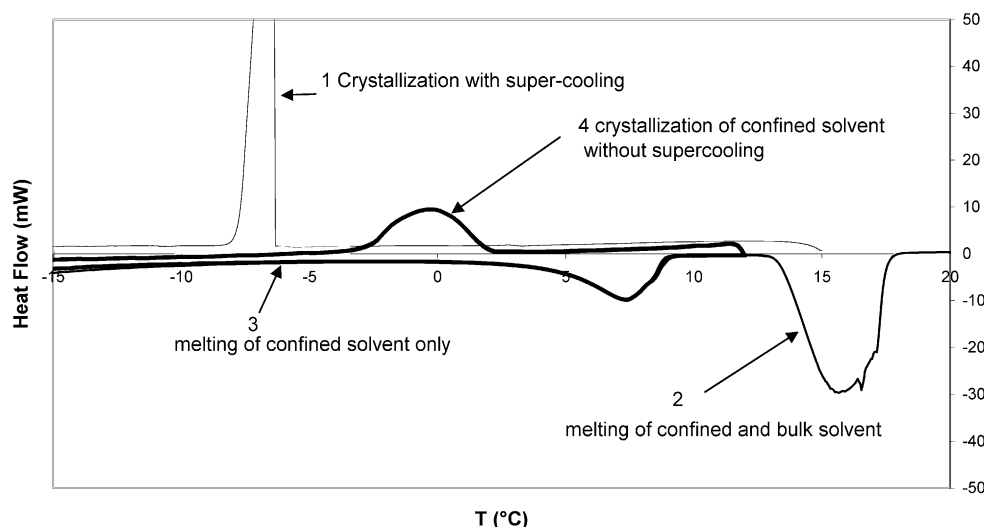


Figure 1. DSC thermograms of 13.5-nm gel soaked in *p*-xylene. 1, the first cooling, showing a dramatic supercooling phenomenon; 2, the direct heating showing the two endothermic peaks; 3, the second heating stopped just before the bulk solvent melts; 4, cooling showing the peak of the trapped *p*-xylene inside the silica gel.

solvents belonging to this family. This work focuses on benzene derivatives and includes the three xylene isomers, paradichlorobenzene, 1,2,4-trichlorobenzene, toluene, and naphthalene. Calibration curves have been determined for all of these solvents by using silica gels with controlled texture. Data collected for the three xylene isomers have then been used as a basis for predictive use of thermoporosimetry with the other solvents.

2. Materials and Methods

All solvents (*o*-, *m*-, and *p*-xylene, *p*-dichlorobenzene, 1,2,4-trichlorobenzene, naphthalene, and toluene) were supplied by Aldrich company and were of high-performance liquid chromatography grade. No further purification was performed.

Nanoporous silica gels were used as standard materials for thermoporosimetry. They were prepared by sol-gel chemistry with tetraethyl-*o*-silicate (TEOS) as a precursor and following procedures described elsewhere.¹⁸ Careful control of the heat treatment leading to the densification of the materials offers the possibility of controlling, to some extent, the final texture of the materials. The materials used in this study are the same as reported in previous work.¹⁶ Textural data of the reference samples were measured by nitrogen sorption on a Quantachrome Autosorb6 and are displayed in Table 1.

TABLE 1: Textural Data of the Nanoporous Silica Gels

sample	V_p (cm ³ /g)	σ (cm ³ /g)	R_p (nm)	σ (nm)
2.5 nm	0.696	0.028	2.40	0.30
3.75 nm	0.922	0.082	3.42	0.67
10.0 nm	0.991	0.071	8.70	1.24
13.5 nm	1.327	0.072	14.25	1.41

To validate the measurements, a control alumina sample supplied by the Coulter Company was used. Its textural data ($S = 212.8$ m²/g, $V = 0.510$ cm³/g) were determined by nitrogen sorption on a Coulter BET SA3100 apparatus.

DSC measurements have been performed on a Mettler Toledo DSC 30 apparatus equipped with a liquid nitrogen cooling system allowing work between -150 and 600 °C. The DSC apparatus was calibrated (both for temperature and enthalpy) with metallic standards (In, Pb, Zn), and the STARE software (Mettler Toledo) was used to calculate temperatures and transition heats from the thermal DSC curves.

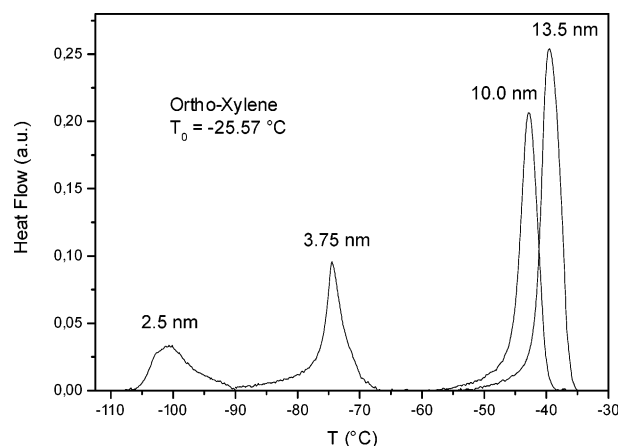


Figure 2. Thermograms recorded for *o*-xylene confined in the four nanoporous silica gels showing clearly the evolution of ΔT as a function of R_p .

3. Theoretical Basis

The phase transition temperature of a solvent, which is confined inside a divided medium, depends on the curvature of the solid/liquid interface. In a porous solid, this curvature is representative of the radius of the pore in which the phase transition takes place. Brun and co-workers have established the theoretical basis of this dependence.⁵ The consequence is that the crystallization temperature T_0 of the solvent undergoes a depression (ΔT) that is related to R_p , the radius of the pore where the phase transition occurs. For the solvents used in this study, this dependence can be expressed as follows

$$R_p = t \exp\left(\frac{-1}{c\Delta T}\right) \quad (1)$$

where R_p is the pore radius, $\Delta T = T_p - T_0$ is the freezing-point depression with T_0 being the crystallization temperature of the pure solvent and T_p the crystallization temperature for the solvent confined in the pore, and t and c are constants depending on the solvent. From this equation

$$\lim_{\Delta T \rightarrow +\infty} (R_p) = t \quad (2)$$

The constant t can consequently be interpreted as the thickness

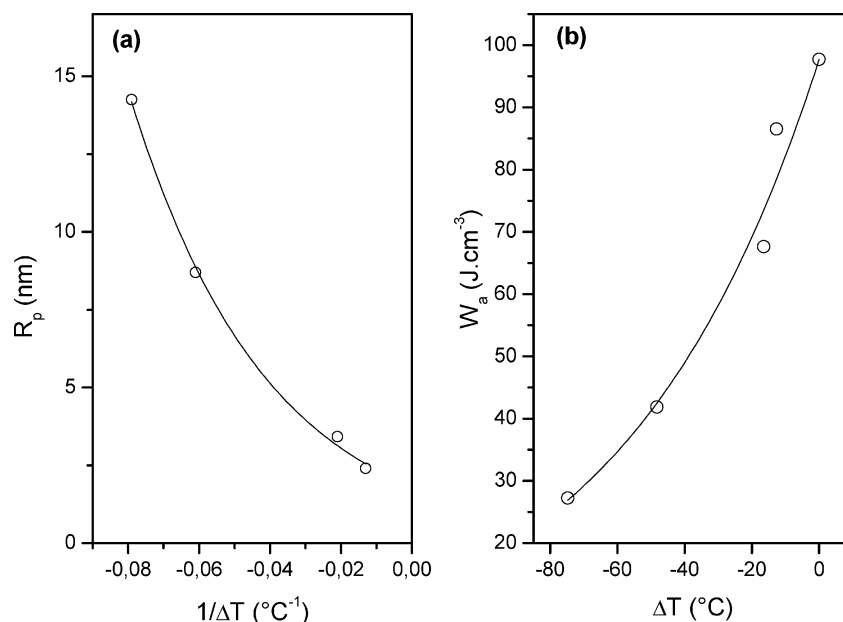


Figure 3. $R_p(1/\Delta T)$ (a) and $W_a(\Delta T)$ (b) curves for *o*-xylene and their corresponding fitting using exponential functions. The point at $\Delta T = 0$ on curve b corresponds to the free solvent.

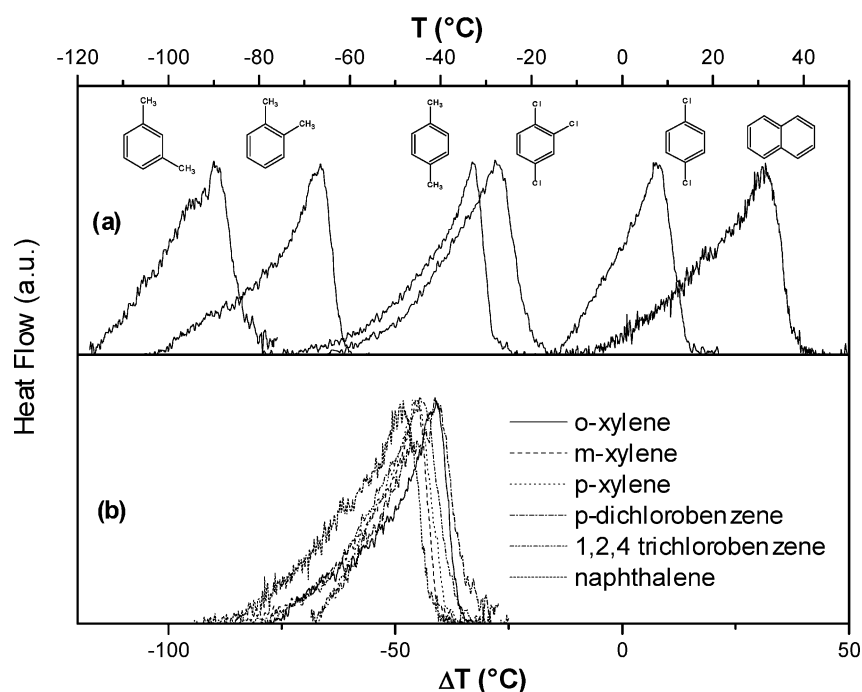


Figure 4. Thermograms recorded for the test alumina sample with various solvents in the T (a) and ΔT (b) scales.

of the layer of solvent remaining adsorbed on the surface of the pore that does not take part in the crystallization.³

Besides, it is possible to calculate the pore-size distribution from the DSC thermal curve obtained from the freezing of the solvent confined inside the pores. Indeed, the pore volume in which the crystallization has occurred can be calculated as follows

$$dV_p = \frac{kY(T) d(\Delta T)}{W_a} \quad (3)$$

where V_p is the pore volume, $Y(T)$ is the DSC thermal curve ordinate (y is baseline corrected), k is a proportionality coefficient depending on the rate of cooling and the sensitivity of

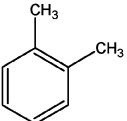
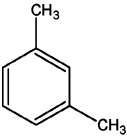
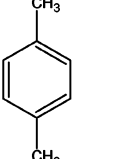
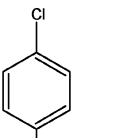
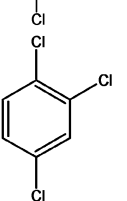
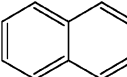
DSC instrument, and W_a is the apparent enthalpy of solidification of the confined solvent.

W_a takes into account the decrease of solidification enthalpy with respect to temperature and the proportion of solvent which does not take part in the crystallization phenomena. One can write

$$W_a = W_{th} \frac{V_p'}{V_p} = W_{th} \frac{\pi l(R_p - t)^2}{\pi l R_p^2} \quad (4)$$

where W_{th} represents the solidification enthalpy of the pure solvent and depends on the phase transition temperature, V_p' is the volume of the solvent really crystallized, V_p is the pore

TABLE 2: Curve-Fitting Parameters for R_p and W_a for *o*-, *m*-, and *p*-Xylene, *p*-Dichlorobenzene, 1,2,4-Trichlorobenzene, and Naphthalene

	t (nm)	c ($^{\circ}\text{C}^{-1}$)	W_0 (J cm^{-3})	f ($^{\circ}\text{C}$)
	1.81	0.0384	97.70	58.0
	1.79	0.0393	98.69	36.3
	1.91	0.0395	117.21	58.5
	1.46	0.0287	151.27	59.7
	1.47	0.0308	140.33	46.3
	1.35	0.0267	134.50	72.3

volume, t is the thickness of the solvent layer that does not crystallize, and l is the cylinder length assuming that the pore shape is cylindrical. Unfortunately W_{th} is not available at T_p , the temperature of crystallization of the solvent inside the pore. However, W_a can be calculated from the DSC thermal curve and the pore volume known by gas sorption for each silica gel sample.

Thus, we can express W_a as follows

$$W_a = \frac{\Delta H}{mV_p} \quad (5)$$

where ΔH is the crystallization enthalpy of the solvent derived from integration of the DSC peak, m is the mass of silica gel dry sample, and V_p is the pore volume per gram of sample.

Finally, it is possible to calculate the pore size distribution (PSD) by combining eqs 1 and 3 to yield

$$\frac{dV_p}{dR_p} = \frac{kY(T)c\Delta T^2}{W_a R_p} \quad (6)$$

Application of eq 6 requires consequently the knowledge of the $W_a(\Delta T)$ and $R_p(\Delta T)$ relationships.

Since no data were available for our solvents, the four nanoporous silica gels described above have been used to get the calibration curves for these solvents. The knowledge of the R_p values (Table 1) and the experimental determination of the corresponding ΔT are indeed sufficient to establish the relation (eq 1), while the knowledge of the porous volume (Table 1)

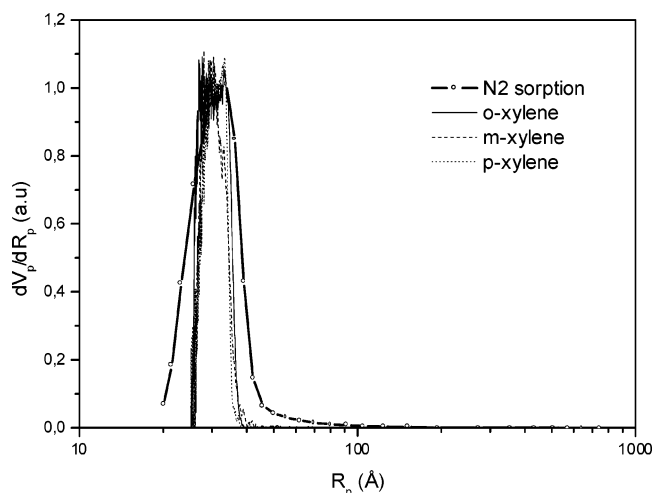


Figure 5. Comparison of PSD of alumina test sample measured from thermoporosimetry with *o*-xylene (solid line), *m*-xylene (dashed line), *p*-xylene (dotted line), and from N_2 gas sorption (O). Distributions are plotted in a log scale for sizes.

and the measurement of the heat of crystallization of the confined solvent at the concerned temperature allow us to reach W_a .

4. Results and Discussion

A monolithic silica gel of about 40 mg is set in a 140- μL DSC pan, and a few solvent drops are added. A visual control, following the spread of the liquid through the sample, is enough to make sure that, after 20 min, the silica is completely saturated. Some extra drops are then added in order to maintain the bulk solvent in a slight excess. Naphthalene and *p*-dichlorobenzene are solids at room temperature. So, after setting the silica pastille in the bottom of the DSC pan, the latter is filled with naphthalene or *p*-dichlorobenzene crystals and then set for 20 min at 85 $^{\circ}\text{C}$ in a thermally regulated oven. The crystals are added until the bulk liquid is in excess, and then the DSC pan is sealed and introduced in the apparatus for thermal analysis. A 0.7 $^{\circ}\text{C}/\text{minute}$ cooling rate was chosen. This cooling rate is slow enough to allow the continuous thermal equilibrium inside the DSC cell.

Despite the weak cooling rate value, a strong supercooling phenomenon is pointed out, making the crystallization peak of the bulk solvent overlap the one of the confined liquid. To avoid this drawback, a particular procedure, illustrated in Figure 1 with the 13.5-nm gel soaked in *p*-xylene, is systematically used especially for the larger pore samples (13.5 and 10.0 nm). The direct cooling (1), from 20 to -20 $^{\circ}\text{C}$ gives a single peak starting at -6 $^{\circ}\text{C}$ and showing a vertical and characteristic shape revealing the breaking of the supercooling.

A first heating (2) is run from -20 up to 20 $^{\circ}\text{C}$, permitting us to record two endothermic peaks: the first one is attributable to the confined *p*-xylene and the second one reveals the fusion of the bulk solvent. A second heating (3) is stopped at 12 $^{\circ}\text{C}$ just after the confined solvent was melted followed by a cooling (4), decreasing the temperature down to -20 $^{\circ}\text{C}$. While temperature decreases, only the confined solvent crystallizes, given that the bulk one is already under solid state. In addition, the crystals of the solid bulk solvent provoke the nucleation inside the confined liquid preventing the supercooling phenomenon.

Two kinds of data can be derived from the (4) DCS thermal curve: the peak position temperature (T) leading to the ΔT calculation and the area under the peak (ΔH (J)), permitting us

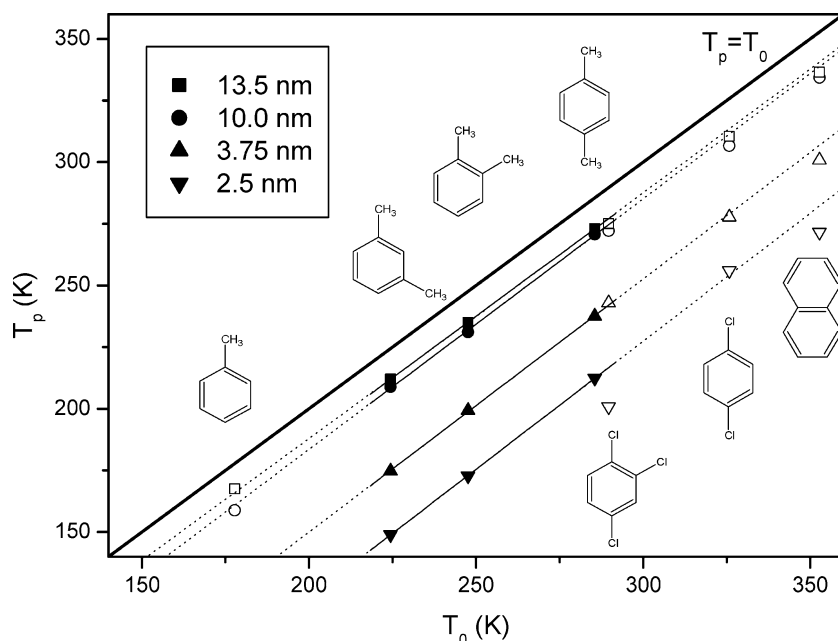


Figure 6. ■, 13.5 nm; ●, 10.0 nm; ▲, 3.75 nm; ▼, 2.5 nm. Continuous lines correspond to the three xylene isomers. Dotted lines represent extension of the fit to the other solvents. The bold line corresponds to the $T_p = T_0$ line, which would correspond to infinite pore size.

to calculate the apparent energy (W_a (J/cm³)) as follows

$$\Delta T = T_p - T_0$$

$$W_a = \frac{\Delta H}{mV_p}$$

where T_0 (°C) is the melting temperature of the bulk solvent, m (g) is the mass of the dry silica gel sample, and V_p (cm³/g) is its porous volume.

For the smaller R_p values, the confined peak is over the breaking supercooling peak and a direct cooling is generally enough.

As an example, the thermograms obtained for the whole series of silica gels with *o*-xylene are displayed in Figure 2. From these curves, it is possible to derive the $R_p(\Delta T)$ and $W_a(\Delta T)$ relations.

Figure 3 shows the plots of R_p vs $1/(\Delta T)$ and W_a vs ΔT for *o*-xylene. For all solvents, fitting of the experimental data is best achieved with an exponential growth model for W_a and an exponential decay for R_p . Fitting has been performed with a least-squares refinement procedure. The corresponding equations are thus

$$R_p = t \exp\left(\frac{-1}{c\Delta T}\right) \quad (1)$$

$$W_a = W_0 \exp\left(\frac{\Delta T}{f}\right) \quad (7)$$

In eq 7, W_0 and f are two constants. Following this equation when $\Delta T = 0$, $W_a = W_0$. W_0 is consequently the enthalpy of crystallization at T_0 . This value can be derived from the DSC thermogram and has been fixed in the fitting procedure.

Table 2 gives the parameters t , c , W_0 , and f determined by fitting the experimental data with the above-mentioned equations for the six solvents.

Knowing these calibration curves for the six solvents, we can now measure PSD by thermoporosimetry using these solvents. To check the reliability of this approach, we have performed measurements of PSD for the test alumina sample using these six solvents.

TABLE 3: Linear-Fit Parameters for the $T_p = f(T_0)$ Curves Corresponding to the Four Silica Gels

R_p (nm)	a	b (K)	R^2
13.5 nm	0.9988	-12.191	1
10.0 nm	1.0161	-19.708	0.9996
3.75 nm	1.0269	-55.452	0.9998
2.5 nm	1.0389	-84.287	1

The thermograms are displayed in Figure 4. In Figure 4a, raw thermograms are displayed in the T scale, while Figure 4b is displayed in the ΔT scale. The shape of the PSD is identical whatever the solvent used, and in the ΔT scale, a good agreement is observed between all measurements. Figure 5 proposes a comparison of PSD determined by thermoporosimetry using the three xylene isomers and the one derived from nitrogen gas sorption. A good agreement is observed between all measurements, thus validating the calibrations performed on the xylenes.

From Figure 4, it is observed that the shift of the freezing temperature, ΔT , whatever the solvent, seems to depend essentially on the value of R_p . To clarify this dependence, Figure 6 shows the plot of T_p (freezing temperature in the pore with radius R_p) vs T_0 (normal freezing temperature of the bulk solvent) for the three xylene isomers. Because of their strong structural similarity, these three solvents are expected to present a similar behavior. The freezing temperatures of the three xylene isomers, confined inside the four nanoporous silica gels (2.5, 3.75, 10.0, and 13.5 nm) are represented by full symbols. For each silica sample, a linear relationship, $T_p = aT_0 + b$, with an excellent correlation coefficient, is found (see Table 3).

The slopes labeled a , of these straight lines, are practically equal to the unit, and no significant dependence on the sample radii is pointed out. On the other hand, the intercepts, b , are largely varying with the degree of division of the medium in which crystallization takes place. These straight lines were extended toward the high- and low-temperature domains, and empty labels representing naphthalene, *p*-dichlorobenzene, 1,2,4-trichlorobenzene, and toluene have been added. All the points obtained for these chemicals are well distributed around the straight lines derived from the xylene data. This is the first evidence of a possible extrapolation of thermoporosimetry data

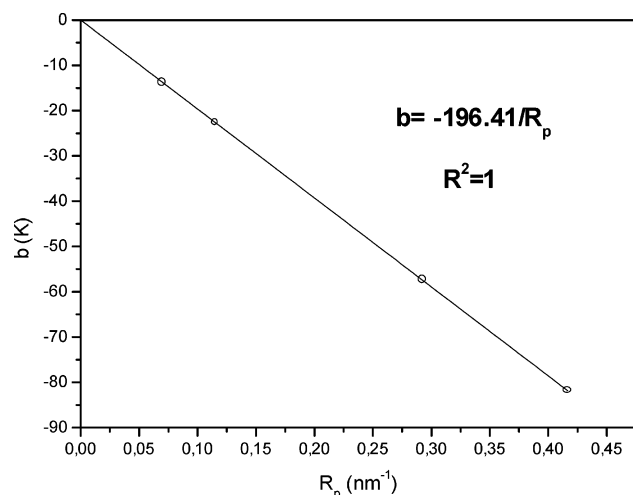


Figure 7. Evolution of parameter b as a function of $1/R_p$ and corresponding linear fit. Equations of the fitting curve and correlation coefficient are also given on the graph.

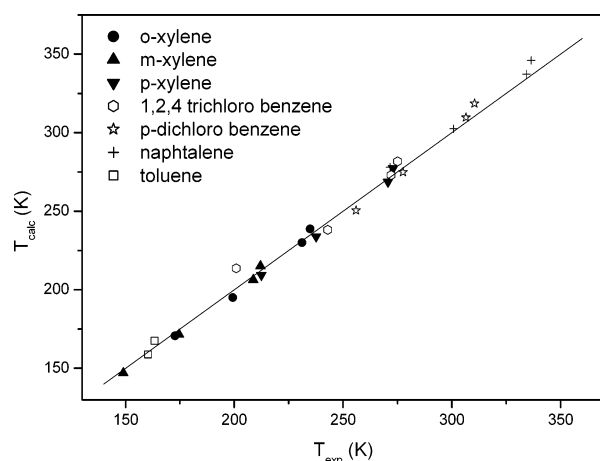


Figure 8. Plot of T_{calc} calculated with eq 7 as a function of T_{exp} measured for the various nanoporous gels and the different solvents. The $y = x$ line is drawn as a guide, and all points are well distributed along this line.

for unknown solvents by the simple knowledge of their melting temperature T_0 . These solvents have been selected due to their chemical and structural similarity with xylene. In effect, all these solvents can indeed be regarded as substituted benzenes.

It has been shown in Table 3 that the intercept, b , of these straight lines depends clearly on the pore size R_p . This dependency is illustrated in Figure 7. A linear evolution of b as a function of $1/R_p$ is observed as attested by the linear fit displayed in Figure 7.

Combining the results derived from Table 3 and Figure 7, the following numerical expression can be proposed allowing prediction of the freezing temperature point of a benzene substituted solvent with T_0 as normal melting temperature and confined inside a divided medium with R_p as pore radius

$$T_p = 1.02T_0 - 196.41/R_p \quad (8)$$

T_p and T_0 are in Kelvin, and R_p is in nm. The 1.02 value is the

average of the slopes of the four straight lines corresponding to the four silica samples for the three xylene isomers. Of course, for high values of R_p (no confinement), eq 8 gives $T_p \approx T_0$.

To check the validity of this approach, freezing points of all the solvents were calculated using the previous equation (T_{calc}) and compared to their experimental values (T_{exp}). A very nice agreement is found as can be seen in Figure 8 where the straight line corresponds to the $T_{\text{calc}} = T_{\text{exp}}$ curve.

So eq 8 is suitable to predict the freezing temperatures of the solvents with a strong structural similarity with xylene, for example, substituted benzenes. Further ongoing work will use this approach for linear alkanes.

5. Conclusion

We have demonstrated in this work that the main limitation of thermoporosimetry, namely, the lack of thermodynamical data on solvents, can be avoided by our new approach. Calibration performed for a few solvents belonging to the general family of substituted benzenes yields a general law which relates the solvent freezing temperature inside a pore of radius R_p to the normal freezing temperature T_0 which is known. This work offers the possibility to use thermoporosimetry on rigid porous materials or polymers directly, without preliminary fastidious calibration. Of course, the general law proposed here has been validated only for some solvents belonging to a specific family. Nevertheless, this could be the starting point for a more efficient, cheaper, and more practical way of using thermoporosimetry. Extension of this work to new families of solvents and toward applications on sol–gel-derived organic–inorganic hybrid materials is underway.

References and Notes

- (1) Thomson, W. *Phil. Mag.* **1871**, 42, 448.
- (2) Patrick, W. A.; Kemper, W. A. *J. Phys. Chem.* **1937**, 42 (3), 369.
- (3) Jackson, C. L.; McKenna, G. B. *J. Chem. Phys.* **1990**, 93 (12), 9002.
- (4) Jackson, C. L.; McKenna, G. B. *Rubber Chem. Technol.* **1991**, 64 (5), 760.
- (5) Brun M.; Lallemand A.; Quinson J.-F.; Eyraud C. *Thermodynam. Acta* **1977**, 21, 59.
- (6) Kim, K. J.; Fane, A. C.; Ben Aim, R.; Lui, M. G.; Jonsson, G.; Tessaro, I. G.; Broek, A. P.; Bargeman, D. J. *Membr. Sci.* **1994**, 87, 35.
- (7) Lui, J.; Gan, L. M.; Chem, C. H.; Teo, W. K.; Gan, L. H. *Langmuir* **1997**, 13, 3 (1), 6421.
- (8) Ishikiriyama, K.; Todoki, M.; Min, K. H.; Yonemori, S.; Noshiro, M. *J. Therm. Anal. Calorim.* **1996**, 46, 1177.
- (9) Larbot, A.; Laaziz, I.; Marignan, J.; Quinson, J. F. *J. Non-Cryst. Solids* **1992**, 147–148, 157.
- (10) Ishikiriyama, K.; Todoki, M. *J. Colloid Interface Sci.* **1995**, 171, 103.
- (11) Neffati, R.; Apekis, L.; Rault, J. *J. Therm. Anal. Calorim.* **1998**, 54, 741.
- (12) Luukkonen, P.; Maloney, T.; Rantanen, J.; Paulapuro, H.; Ylruusi, J. *Pharm. Res.* **2001**, 18, 1562.
- (13) Drouin, J. M.; Chopin, T.; Nortier, P.; Van Damme, H. *J. Colloid Interface Sci.* **1988**, 125, 314.
- (14) Baba, M.; Nedelec, J. M.; Lacoste, J.; Gardette, J. L. *J. Non-Cryst. Solids* **2002**, 315, 228.
- (15) Baba, M.; Nedelec, J.-M.; Lacoste, J.; Gardette, J. L.; Morel M. *Polym. Degrad. Stab.* **2003**, 80 (2), 305.
- (16) Baba M.; Gardette, J. L.; Lacoste, J. *Polym. Degrad. Stab.* **1999**, 65, 415.
- (17) Baba M.; Nedelec, J.-M.; Lacoste, J. *J. Phys. Chem. B* **2003**, 107, 12884.
- (18) Hench, L. L. In *Sol–gel silica: processing, properties and technology transfer*; Noyes Publications: New York, 1998.